Tumor susceptibility gene 101 ameliorates endotoxin-induced cardiac dysfunction by enhancing Parkin-mediated mitophagy

Received for publication, April 16, 2019, and in revised form, October 10, 2019 Published, Papers in Press, October 16, 2019, DOI 10.1074/jbc.RA119.008925

Kobina Essandoh[‡1], Xiaohong Wang[‡1], Wei Huang[§], Shan Deng[‡¶], George Gardner[‡], Xingjiang Mu[‡], Yutian Li[‡], Evangelia G. Kranias[‡], Yigang Wang[§], and Guo-Chang Fan[‡2]

From the Departments of [‡]Pharmacology and Systems Physiology, [§]Pathology and Laboratory Medicine, University of Cincinnati College of Medicine, Cincinnati, Ohio 45267 and the [¶]Department of Cardiology, Union Hospital, Tongji Medical College, Huazhong University of Science and Technology, Wuhan 430022, China

Edited by Phyllis I. Hanson

Cardiac mitochondrial damage and subsequent inflammation are hallmarks of endotoxin-induced myocardial depression. Activation of the Parkin/PTEN-induced kinase 1 (PINK1) pathway has been shown to promote autophagy of damaged mitochondria (mitophagy) and to protect from endotoxin-induced cardiac dysfunction. Tumor susceptibility gene 101 (TSG101) is a key member of the endosomal recycling complexes required for transport, which may affect autophagic flux. In this study, we investigated whether TSG101 regulates mitophagy and influences the outcomes of endotoxin-induced myocardial dysfunction. TSG101 transgenic and knockdown mice underwent endotoxin/lipopolysaccharide treatment (10 μg/g) and were assessed for survival, cardiac function, systemic/local inflammation, and activity of mitophagy mediators in the heart. Upon endotoxin challenge and compared with WT mice, TSG101 transgenic mice exhibited increased survival, preserved cardiac contractile function, reduced inflammation, and enhanced mitophagy activation in the heart. By contrast, TSG101 knockdown mice displayed opposite phenotypes during endotoxemia. Mechanistically, both coimmunoprecipitation assays and coimmunofluorescence staining revealed that TSG101 directly binds to Parkin in the cytosol of myocytes and facilitates translocation of Parkin from the cytosol to the mitochondria. Our results indicate that TSG101 elevation could protect against endotoxin-triggered myocardial injury by promoting Parkin-induced mitophagy.

Sepsis, which is defined by consensus as a dysregulated host response to infection, remains a major contributor to mortality in intensive care units of hospitals (1). Sepsis-induced mortality has primarily been ascribed to multiple organ dysfunction, of which cardiac contractile dysfunction has been linked with increased risk of mortality (2, 3). The active outer membrane phospholipid component of Gram-negative bacteria, endotoxin (lipopolysaccharide (LPS)),[3] has been implicated as a major causative factor for sepsis-induced cardiomyopathy (4, 5). Endotoxin is able to either bind with plasma membrane receptors (*i.e.* Toll-like receptors) or infiltrate into intracellular spaces, where it can interfere with organelle function (6). Although the exact mechanisms of such actions remain obscure, endotoxin-triggered myocardial depression has been largely attributed to mitochondrial dysfunction, pro-inflammatory cytokines/mediators, and nitric oxide production (6).

Currently, it is well recognized that mitochondrial function and quality control are extremely essential for cardiomyocyte contractile function (7). In general, mitochondrial quality control is maintained by the ubiquitin-proteasome system, selective autophagy of damaged mitochondria (mitophagy), and mitochondrial biogenesis (8). Disruption of these processes contributes to the pathophysiology of various cardiovascular disorders (9, 10). Endotoxin-induced mitochondrial impairment has been well established in human septic patients and septic animal models (11–14). However, therapies targeting mitochondrial dysfunction in septic patients have not been explored. Recent studies in mice and rats have demonstrated that activation of mitophagy could greatly rescue LPS-induced cardiac dysfunction (15, 16). At present, it is well established that mitophagy is regulated by the E3 ubiquitin ligase Parkin (17) and the mitochondrial serine-threonine kinase PTEN-induced putative kinase 1 (PINK1) (18). When the mitochondria are depolarized and damaged, PINK1 recruits cytosolic Parkin to the mitochondria, which, in turn, drives the damaged mitochondria to microtubule-associated protein 1A/1B light chain 3 (LC3) to be degraded and regenerated by autolysosomes (19). Parkin-deficient mice showed multiple cardiac mitochondrial defects and worse cardiac contractile function compared with WT mice when challenged with endotoxin (20). Thus, targeting

This study was supported in part by National Institutes of Health grants R01 GM-126061 and GM-132149 and American Heart Association Established Investigator Award 17EIA33400063 (to G.-C. F.) and American Heart Association Predoctoral Fellowship 18PRE34030123 (to K. E.). The authors declare that they have no conflicts of interest with the contents of this article. The content is solely the responsibility of the authors and does not necessarily represent the official views of the National Institutes of Health.
This article contains Figs. S1–S3 and Tables S1–S3.

[1] Both authors contributed equally to this work.
[2] To whom correspondence should be addressed: Dept. of Pharmacology and Systems Physiology, University of Cincinnati College of Medicine, 231 Albert Sabin Way, Cincinnati, OH 45267-0575; Tel.: 513-558-2340; Fax: 513-558-9969; E-mail: fangg@ucmail.uc.edu.

[3] The abbreviations used are: LPS, lipopolysaccharide; TG, transgenic; TNF, tumor necrosis factor; NRCM, neonatal rat cardiomyocyte; mtDNA, mitochondrial DNA; mtROS, mitochondrial reactive oxygen species; MPO, myeloperoxidase; KD, knockdown; CTRL, control; UEV, ubiquitin E2 variant; MHC, major histocompatibility complex; RT-qPCR, quantitative RT-PCR.

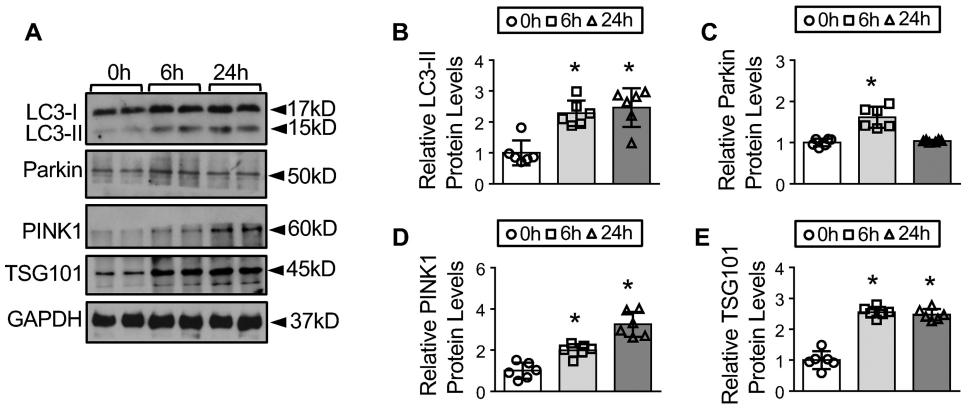

Figure 1. Endotoxin activates mitophagy in the mouse heart together with up-regulation of TSG101. *A–E*, Western blots and quantification analysis (*A*) showing the differential expression of LC3-II (*B*), Parkin (*C*), PINK1 (*D*), and TSG101 (*E*) in hearts of mice subjected to endotoxin injection for 0, 6, and 24 h. GAPDH was used as a loading control for total protein. $n = 6$ for all groups. *, $p < 0.05$ *versus* 0 h.

the Parkin/PINK1 pathway and mitochondrial autophagy (mitophagy) may provide the best outcomes in sepsis.

Tumor susceptibility gene 101 (TSG101) was originally linked to breast cancer (21, 22). Later, several groups identified TSG101 as an essential member of the endosomal complex required for transport (23). Most importantly, studies have also suggested that knockdown of TSG101 results in accumulation of autophagosomes and defective autophagic flux in various cancer cell lines (24, 25). Recently, we showed that TSG101 can promote endosomal recycling of insulin-like-growth factor 1 (IGF-1R) in cardiomyocytes and positively regulate physiological cardiac hypertrophy (26). However, the definitive role of TSG101 in cardiac selective autophagy of damaged mitochondria (mitophagy) during endotoxemia remains unknown. Hence, it would be intriguing to elucidate whether TSG101 regulates mitophagy and its consequences for endotoxin-induced cardiac dysfunction.

In this study, we first observed that mitophagy was activated in mouse hearts when challenged with endotoxin, which coincided with up-regulation of TSG101 protein levels. Mice with cardiac-specific overexpression of TSG101 were resistant to endotoxin-triggered mortality, cardiac dysfunction, and inflammation. On the other hand, endotoxin treatment in mice with inducible cardiac-specific knockdown of TSG101 exaggerated mortality, myocardial dysfunction, inflammation, and mitochondrial damage. Mechanistically, we identified that TSG101 could interact with Parkin, which promoted translocation of Parkin from the cytosol to mitochondria in endotoxemic cardiomyocytes.

Results

Endotoxin activates mitophagy in the mouse heart together with up-regulation of TSG101

Mitophagy has been demonstrated to play a protective role in the heart during endotoxin challenge (15, 16). Notably, Parkin and PINK1, two major players of mitophagy, are essential for its protection against endotoxin-induced cardiac impairment (20). To determine the expression pattern of mitophagy mediators (*i.e.* Parkin and PINK1) and the autophagic flux marker LC3-II in endotoxemic hearts, LPS was injected i.p. into mice, and heart samples were collected after 0, 6, and 24 h for Western blot analysis. We observed that cardiac LC3-II protein levels were significantly up-regulated 6 h and 24 h post-injection (Fig. 1, *A* and *B*), suggesting that treatment of mice with LPS led to increased autophagy flux in the heart. Interestingly, protein levels of Parkin were greatly increased at 6 h but returned to basal levels 24 h post-LPS injection (Fig. 1, *A* and *C*), suggesting early activation of Parkin in endotoxemic hearts. Similar to LC3-II, cardiac protein levels of PINK1 were continuously elevated 6 and 24 h post-LPS injection (Fig. 1, *A* and *D*). Considering that previous reports indicated a possible contribution of TSG101 to autophagy in cancer cells (24, 25), we next sought to determine whether TSG101 protein levels were dysregulated in mouse hearts upon endotoxin treatment. Immunoblot analysis results showed that TSG101 protein levels were remarkably increased in mouse hearts 6 and 24 h after LPS injection (Fig. 1, *A* and *E*). These results indicate that TSG101 may play a role in cardiac response to endotoxin stress and that the increase of TSG101 may be linked to Parkin/PINK1-mediated mitophagy.

Overexpression of TSG101 improves animal survival and cardiac function and reduces inflammation upon endotoxin challenge

To investigate the possible role of TSG101 in endotoxin-induced cardiac dysfunction, a transgenic mouse model with cardiac-specific overexpression of TSG101 was generated (26). We selected the G line of the TSG101 transgenic (TG) mouse model for the following experiments (Fig. 2*A*), as this line of TG hearts showed ~4-fold overexpression of TSG101 compared with WT hearts (Fig. 2*B*), which was close to the magnitude of up-regulation of TSG101 in LPS-treated mouse hearts (Fig. 1, *A* and *E*). Given that endotoxin can cause myocardial depression and animal death (13, 14), we first monitored survival rates in TSG101-TG mice and WT controls over 5 days after LPS injection. Survival analysis results showed a higher survival rate in TG mice (six of seven TG mice survived) after endotoxin challenge, whereas only three of eight WT mice survived (Fig. 2*C*). Consistent with previous reports (13, 14), cardiac function parameters, ejection fraction, and fractional shortening were significantly decreased in LPS-treated WT mice (Fig. 2, *D–F*, and Table S1). However, cardiac function was preserved in LPS-treated TG mice (Fig. 2, *D–F*, and Table S1). Considering that

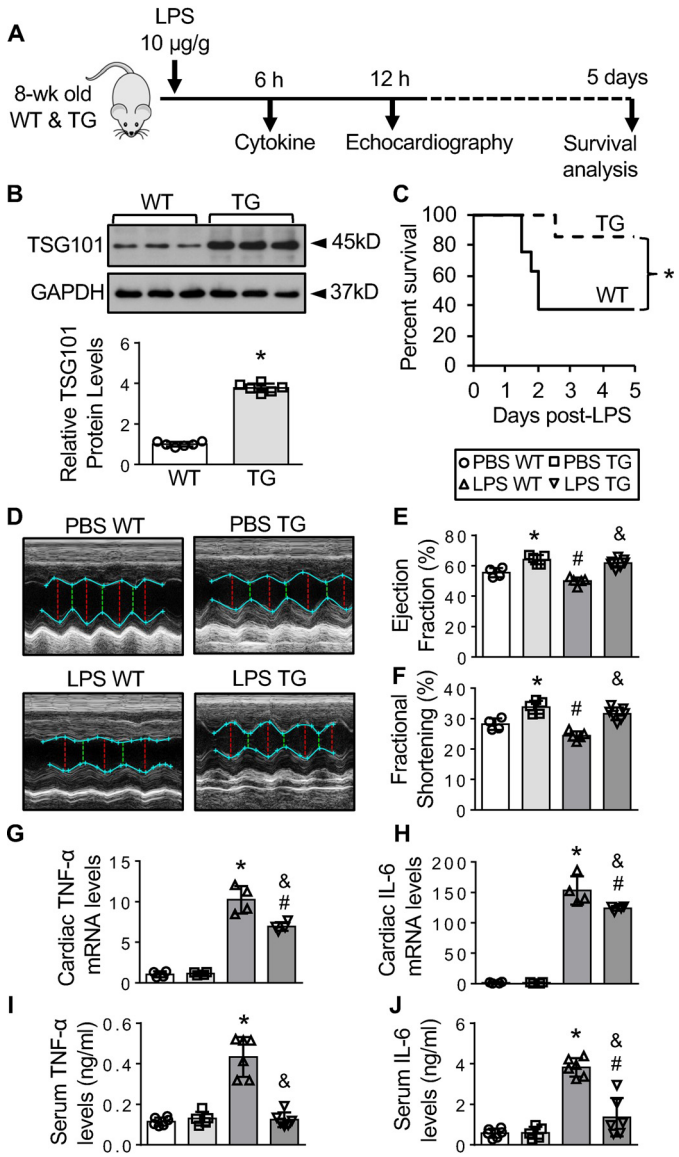

Figure 2. Overexpression of TSG101 improves animal survival and cardiac function and reduces inflammation upon endotoxin challenge. *A*, experimental procedure and biochemical assays for LPS (10 μg/g) treatment in WT and TG mice. *wk*, week. *B*, Western blots and quantification analysis showing the expression of TSG101 in hearts of WT and TG mice. GAPDH was used as a loading control for total protein. $n = 6$ for all groups. *, $p < 0.05$ *versus* WT. *C*, survival curve of WT and TG mice when challenged with LPS (10 μg/g) and monitored over 5 days. $n = 8$ for WT, $n = 7$ for TG. *, $p < 0.05$ *versus* WT. *D–F*, cardiac function in WT and TG mice subjected to PBS or LPS treatment was determined by echocardiography. $n = 4$ for PBS WT, $n = 5$ for PBS TG, $n = 5$ for LPS WT, $n = 7$ for LPS TG. * and #, $p < 0.05$ *versus* PBS WT; &, $p < 0.05$ *versus* LPS WT. *G* and *H*, levels of the pro-inflammatory cytokines TNFα (*G*) and IL-6 (*H*) in WT and TG mice subjected to PBS or LPS treatment were determined by qRT-PCT. $n = 4$ for all groups. *, $p < 0.05$ *versus* PBS WT; #, $p < 0.05$ *versus* PBS TG; &, $p < 0.05$ *versus* LPS WT. *I* and *J*, levels of the pro-inflammatory cytokines TNFα (*I*) and IL-6 (*J*) in WT and TG mice subjected to PBS or LPS treatment were measured by ELISA. $n = 6$ for all groups. *, $p < 0.05$ *versus* PBS WT; #, $p < 0.05$ *versus* PBS TG; &, $p < 0.05$ *versus* LPS WT.

endotoxin-induced mortality and cardiac dysfunction have been ascribed to elevation of systemic/local inflammation (1, 4), we next measured the levels of pro-inflammatory cytokines in the sera and cardiac tissues of LPS-injected mice (Fig. 2*A*). Quantitative PCR and ELISA results showed that cardiac and systemic levels of TNFα and IL-6 were greatly increased in LPS-treated WT mice, but this increase was significantly attenuated in LPS-treated TG mice (Fig. 2, *G–J*). Given that the TSG101-TG model is cardiomyocyte-specific, we were curious about why circulating cytokines were reduced in this mouse model. As reported previously by our laboratory, elevation of TSG101 in cardiomyocytes can promote exosome release, which may affect remote or neighboring cells through transfer of encapsulated content (27). Therefore, we speculated that such systemic effects of TSG101-TG hearts on circulating immune cells (*i.e.* macrophages) might be partly ascribed to exosomes released by TSG101-overexpressing cardiomyocytes. To confirm this possibility, we utilized an *in vitro* approach to isolate exosomes from neonatal rat cardiomyocytes (NRCMs) transfected with the adenovirus vector Ad.TSG101 or control Ad.GFP. We observed that protein levels of the exosomal marker CD63 were elevated together with higher levels of TSG101 in equal amounts of exosomes (20 μg) isolated from Ad.TSG101 NRCMs (TSG101-exo) compared with those collected from Ad.GFP NRCMs (GFP-exo), although the average sizes of both sets of exosomes were similar (Fig. S1, *A–C*). Importantly, RAW264.7 macrophages treated with TSG101-exo showed higher levels of TSG101, Parkin, and PINK1 under both PBS- and LPS-stimulated conditions than cells treated with an equal amount of GFP-exo (2 μg/ml) (Fig. S1, *D–G*). Accordingly, treatment of macrophages with TSG101-exo (2 μg/ml) diminished production of the inflammatory cytokine IL-6 compared with GFP-exo–treated cells (Fig. S1*H*). Hence, these results suggest that exosomes released by TSG101-overexpressing cardiomyocytes may have paracrine effects on circulating immune cells. Together, these data indicate that overexpression of TSG101 could protect mice against endotoxin-induced death, cardiac dysfunction, and local/systemic inflammation.

Overexpression of TSG101 enhances mitophagy and mitochondrial integrity in endotoxin-treated hearts

To elucidate whether TSG101-mediated protection against endotoxemia is associated with mitophagy, we next determined the expression levels of the mitophagy regulators Parkin and PINK1 in LPS-treated mouse hearts (Fig. 3*A*). Interestingly, we observed that the protein levels of Parkin and PINK1 were significantly increased in TSG101-TG hearts compared with WT controls under basal conditions (Fig. 3, *B–E*). Notably, overexpression of TSG101 in mouse hearts enhanced the mRNA levels of Parkin, but not PINK1, under basal conditions (Fig. S2, *A–C*). As expected, treatment of mice with LPS enhanced expression of Parkin and PINK1 in WT hearts; however, such increases were more pronounced in TSG101-TG hearts upon LPS challenge (Fig. 3, *B–E*). Accordingly, autophagic flux was significantly enhanced in TSG101-TG hearts, as evidenced by higher levels of LC3-II than in WT hearts under basal and LPS conditions (Fig. 3, *B* and *F*). Remarkably, we found that TSG101 and Parkin levels were decreased in cytosolic fractions in both WT and TG hearts after LPS treatment compared with PBS conditions (Fig. S2, *D* and *F–H*). Conversely, the levels of TSG101, Parkin, and PINK1 were increased in mitochondrial fractions in the hearts of WT and TG mice upon endotoxin challenge, and such elevations were more pronounced in mitochondrial fractions of TG hearts than in WT controls (Fig. S2, *E*

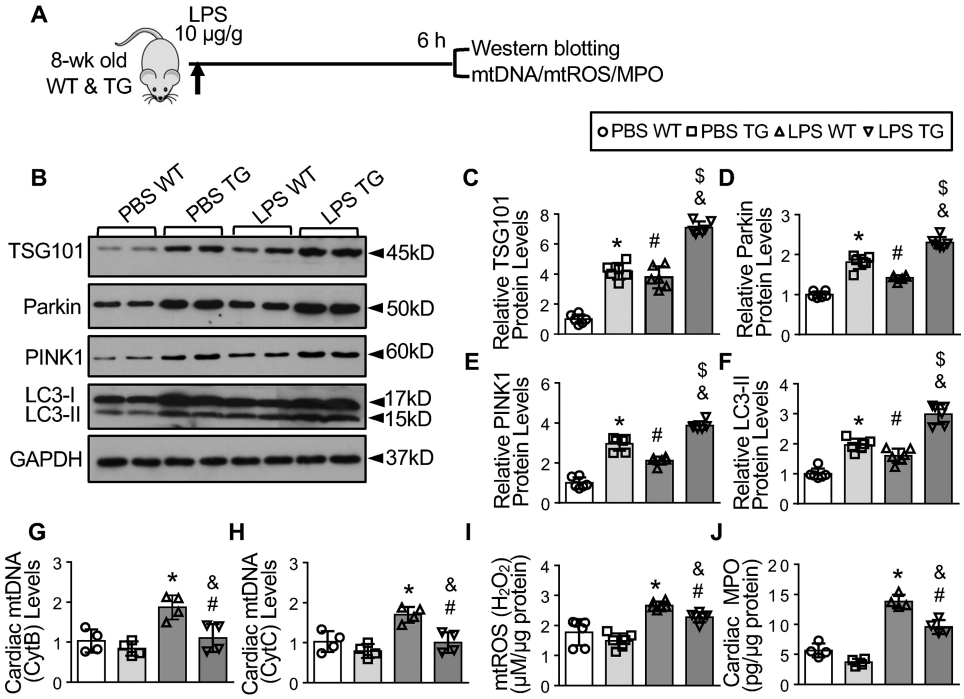

Figure 3. Overexpression of TSG101 enhances mitophagy and mitochondrial integrity in endotoxin-treated hearts. *A*, experimental procedure and biochemical assays for LPS (10 μg/g) treatment in WT and TG mice. *wk*, week. *B*, Western blots and quantification analysis (*B*) showing protein levels of TSG101 (*C*), Parkin (*D*), PINK1 (*E*), and LC3-II (*F*) in hearts of WT and TG mice subjected to endotoxin injection for 6 h. GAPDH was used as a loading control for total protein. $n = 6$ for all groups. * and #, $p < 0.05$ *versus* PBS WT; &, $p < 0.05$ *versus* PBS TG; $, $p < 0.05$ *versus* LPS WT. *G* and *H*, quantification of mtDNA by RT-PCR using primers targeted to mitochondrial cytochrome *b* (*CytB*, *G*) and mitochondrial cytochrome c (*CytC*, *H*) in hearts of WT and TG mice subjected to endotoxin injection for 6 h. $n = 4$ for all groups. *, $p < 0.05$ *versus* PBS WT; #, $p < 0.05$ *versus* PBS TG; &, $p < 0.05$ *versus* LPS WT. *I*, levels of mitochondrial hydrogen peroxide (ROS) in hearts of WT and TG mice subjected to endotoxin injection for 6 h was measured by Amplex Red assay. $n = 6$ for all groups. *, $p < 0.05$ *versus* PBS WT; #, $p < 0.05$ *versus* PBS TG; &, $p < 0.05$ *versus* LPS WT. *J*, levels of MPO in hearts of WT and TG mice subjected to endotoxin injection for 6 h was measured by MPO ELISA kit. $n = 4$ for all groups. *, $p < 0.05$ *versus* PBS WT; #, $p < 0.05$ *versus* PBS TG; &, $p < 0.05$ *versus* LPS WT.

and *I–K*). These data suggest enhanced translocation of TSG101 and Parkin from the cytosol to the mitochondria in TG hearts during endotoxemia. Next we examined whether overexpression of TSG101 affected the release of mitochondrial DNA (mtDNA) and reactive oxygen species (mtROS), two indicators of mitochondrial damage during endotoxemia (15, 28). As shown in Fig. 3, *G–I*, the levels of mtDNA and mtROS were remarkably lower in LPS-TG hearts than in LPS-WT hearts. Further, the levels of myeloperoxidase (MPO), an enzyme released from infiltrating neutrophils because of cellular oxidative stress (28), were significantly lower in LPS-TG hearts compared with LPS-WT hearts (Fig. 3*J*). Collectively, these data suggest that TSG101-elicited protective effects against endotoxemia may be due to enhanced cardiac mitophagy.

Knockdown of TSG101 exacerbates LPS-triggered animal mortality, cardiac dysfunction, and inflammation

To further investigate the role of TSG101 in endotoxin-induced cardiac injury, we utilized an inducible cardiac-specific TSG101 knockdown (KD, MerCreMer-TSG101$^{fl/+}$) mouse model that underwent LPS challenge 1 week after the last injection of tamoxifen (Fig. 4*A*). Complete knockout of TSG101 is lethal (26). Genetic knockdown of TSG101 in the mouse hearts was confirmed by Western blot analysis (Fig. 4*B*). We observed that only two of eight KD mice survived 5 days post-LPS injection, whereas seven of 10 control (CTRL, TSG101$^{fl/+}$) mice survived when challenged with LPS (Fig. 4*C*). Further, under basal conditions, KD mice exhibited similar cardiac contractile function as CTRL mice (Fig. 4, *D–F*, and Table S2). However, the degree of LPS-triggered cardiac dysfunction was greater in KD mice than in CTRL mice, as evidenced by a significantly larger reduction in ejection fraction and fractional shortening in KDs compared with CTRLs, which underwent endotoxemia for 12 h (Fig. 4, *D–F*, and Table S2). Accordingly, there were higher levels of systemic and cardiac pro-inflammatory cytokines, TNF and IL-6, in LPS-treated KD mice than in CTRLs (Fig. 4, *G–J*). Together, these data demonstrate that knockdown of TSG101 in the heart exaggerates endotoxin-triggered mortality, cardiac dysfunction, and inflammation.

Knockdown of TSG101 diminishes mitophagy and mitochondrial integrity in LPS-treated hearts

To determine whether knockdown of TSG101 affected cardiac mitophagy during endotoxemia, we subjected CTRL and KD mice to LPS treatment for 6 h and collected heart samples for Western blotting and quantification of mtDNA, mtROS, and MPO (Fig. 5*A*). Immunoblot analysis showed that knockdown of TSG101 in the heart significantly reduced the protein levels of Parkin, PINK1, and LC3-II under basal (PBS) conditions (Fig. 5, *B–F*), although there were no significant changes in the mRNA levels of Parkin and PINK1 (Fig. S3, *A–C*). Although administration of LPS elicited compensatory up-regulation of PINK1, Parkin, and LC3-II expression in CTRL hearts, up-regulation of these proteins was remarkably attenuated in KD hearts (Fig. 5, *B–F*). Similar to the TG model, endotoxin treatment elicited a reduction in the levels of cytosolic

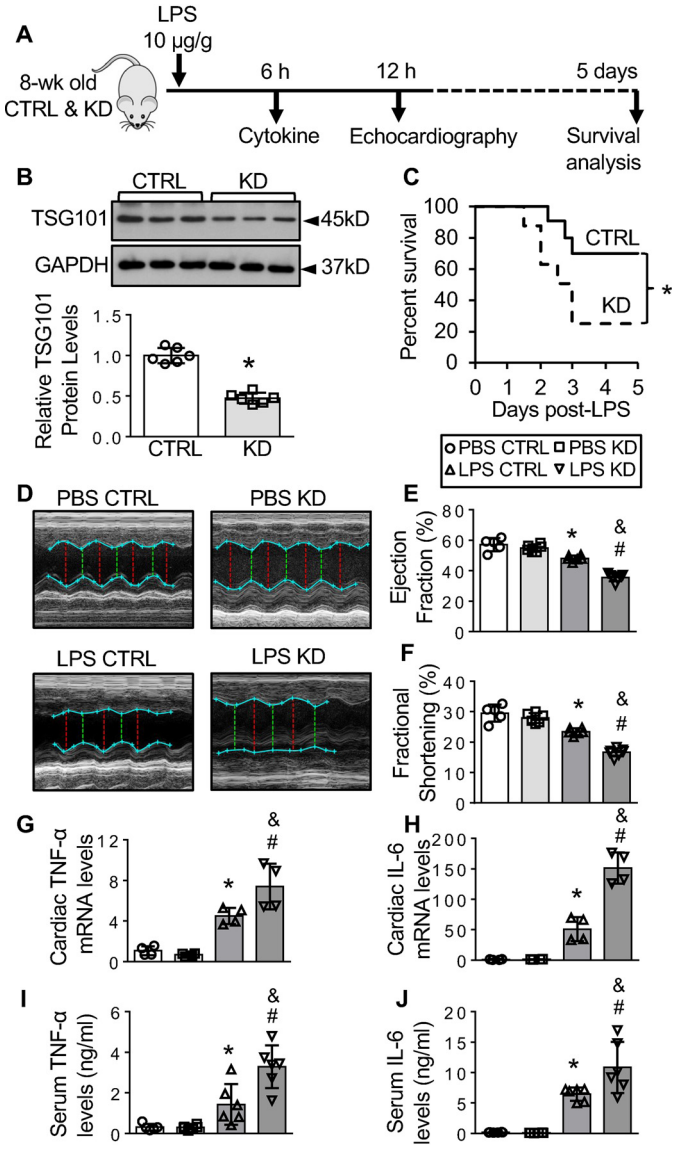

Figure 4. Knockdown of TSG101 exacerbates LPS-triggered animal mortality, cardiac dysfunction, and inflammation. *A*, experimental procedure and biochemical assays for LPS (10 μg/g) treatment in CTRL (TSG101$^{fl/+}$) and TSG101 KD (MerCreMer-TSG101$^{fl/+}$) mice. *wk*, week. *B*, Western blots and quantification analysis showing the expression of TSG101 in hearts of CTRL and KD mice. GAPDH was used as a loading control for total protein. $n = 6$ for all groups. *, $p < 0.05$ *versus* CTRL. *C*, survival curve of CTRL and KD mice when challenged with LPS (10 μg/g) and monitored over 5 days. $n = 10$ for CTRL, $n = 8$ for KD. *, $p < 0.05$ *versus* CTRL. *D–F*, cardiac function in CTRL and KD mice subjected to PBS or LPS treatment was determined by echocardiography. $n = 5$ for PBS CTRL, $n = 6$ for PBS KD, $n = 6$ for LPS CTRL, $n = 7$ for LPS KD. *, $p < 0.05$ *versus* PBS CTRL; #, $p < 0.05$ *versus* PBS KD; &, $p < 0.05$ *versus* LPS CTRL. *G* and *H*, levels of the pro-inflammatory cytokines TNFα (*G*) and IL-6 (*H*) in CTRL and KD mice subjected to PBS or LPS treatment were determined by qRT-PCR. $n = 4$ for all groups. *, $p < 0.05$ *versus* PBS CTRL; #, $p < 0.05$ *versus* PBS KD; &, $p < 0.05$ *versus* LPS CTRL. *I* and *J*, levels of the pro-inflammatory cytokines TNFα (*I*) and IL-6 (*J*) in CTRL and KD mice subjected to PBS or LPS treatment were measured by ELISA. $n = 6$ for all groups. *, $p < 0.05$ *versus* PBS CTRL; #, $p < 0.05$ *versus* PBS KD; &, $p < 0.05$ *versus* LPS CTRL.

TSG101 and Parkin, but there was an elevation in mitochondrial PINK1, Parkin, and TSG101 levels in both CTRL and KD hearts compared with PBS conditions (Fig. S3, *D–K*). Notably, such mitochondrial translocation of PINK1, Parkin, and TSG101 was greatly reduced in KD hearts compared with CTRLs (Fig. S3, *D–K*). In addition, the levels of mtDNA, mtROS, and MPO were much higher in LPS-treated KD hearts than in CTRL hearts (Fig. 5, *G–J*). These data indicate that knockdown of TSG101 significantly inhibits activation of mitophagy in the endotoxemic heart.

TSG101 interacts with and augments the function of Parkin in endotoxin-treated hearts

To elucidate how TSG101 regulates cardiac mitophagy during endotoxemia, we performed coimmunoprecipitation assays using antibodies of TSG101, Parkin, and PINK1 in heart homogenates of WT and TG mice subjected to endotoxin challenge for 6 h. Our results showed that not only did TSG101 bind to Parkin, but this association was further enhanced in both WT and TG hearts after endotoxin challenge (Fig. 6, *A* and *B*). Interestingly, TSG101 did interact with Parkin but did not bind to PINK1 (Fig. 6*A*). As expected, Parkin interacted with PINK1 because such an interaction is well known to target damaged mitochondria to autophagosomes and lysosomes (Fig. 6, *A* and *B*). To further validate that TSG101 interacted with Parkin, we performed coimmunostaining in isolated neonatal rat cardiomyocytes that were treated with PBS or LPS (1 μg/ml) for 3 h. The results of coimmunostaining for mitochondria (MitoTracker), TSG101, and Parkin revealed that a small portion of TSG101 and Parkin were colocalized within mitochondria under the basal (PBS) condition (Fig. 6*C*). However, in LPS-treated cardiomyocytes, a large portion of TSG101 overlapped with Parkin at the mitochondria (Fig. 6*C*). Next we sought to elucidate the specific domain of TSG101 that interacts with Parkin. Human and mouse TSG101 proteins, which are highly conserved between both species, contain four known structural motifs: the N-terminal ubiquitin E2 variant (UEV) domain, proline-rich region, a coiled-coil region, and a C-terminal α-helical/steadiness box domain (Fig. 6*D*) (29). To delineate the essential domain of TSG101 that binds to Parkin, we cotransfected the indicated truncates of myc-tagged human TSG101 plasmids with the mCherry-tagged human Parkin plasmid into HEK293T cells (Fig. 6*D*). Using immunoblot analysis, we confirmed the expression of these transfected plasmids in HEK293T cells (Fig. 6*E*). Coimmunoprecipitation assays demonstrated that TSG101 mutants containing an UEV domain (2, 3, 6, and 7) could bind to Parkin (Fig. 6, *F* and *G*). These results indicate that TSG101 interacts with Parkin through its UEV domain and that such an association may enhance translocation of Parkin from the cytosol to mitochondria after LPS challenge.

TSG101 promotes mitochondrial fission and biogenesis upon endotoxin challenge

Besides mitophagy, mitochondrial structural integrity could be regulated by mitochondrial fusion, fission, and biogenesis (30). Mitochondrial fusion is the merging of mitochondria and is controlled by Mitofusins (Mfn1 and Mfn2) (30). Mitochondrial fission is the process of breaking down damaged mitochondria for easy removal and degradation and is primarily regulated by dynamin-related protein 1 (Drp1) (30). Thus, mitochondrial fission promotes activation of mitophagy, whereas fusion inhibits mitophagy (31). Mitochondrial biogenesis is the replacement of mitochondria that have been

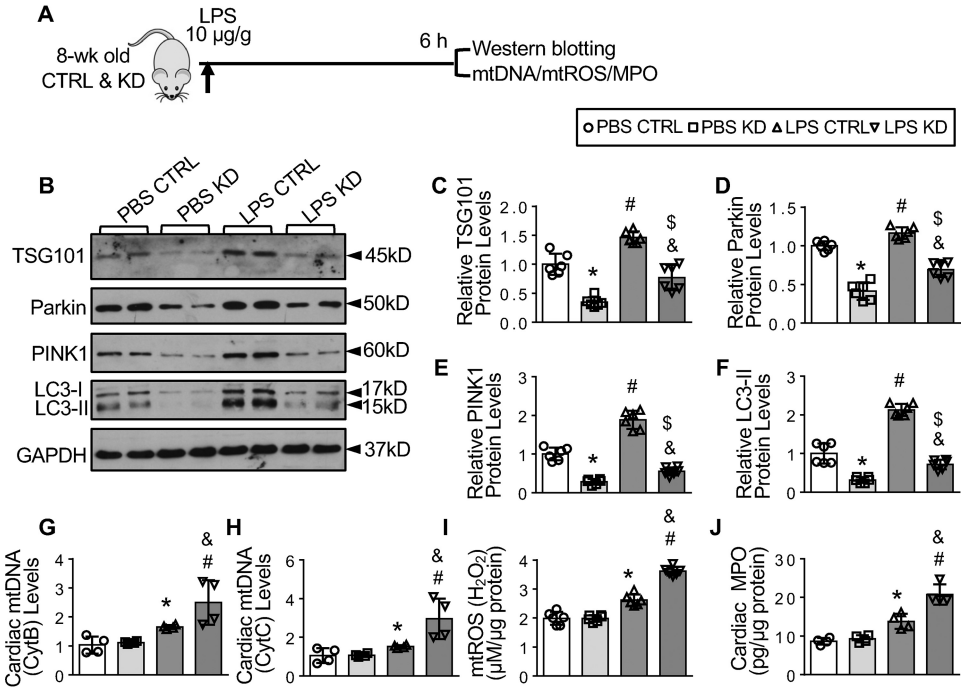

Figure 5. Knockdown of TSG101 diminishes mitophagy and mitochondrial integrity in LPS-treated hearts. *A*, experimental procedure and biochemical assays for LPS (10 μg/g) treatment in CTRL (TSG101$^{fl/+}$) and TSG101 KD (MerCreMer-TSG101$^{fl/+}$) mice. *wk*, week. *B–F* Western blots and quantification analysis (*B*) showing protein levels of TSG101 (*C*), Parkin (*D*), PINK1 (*E*), and LC3-II (*F*) in hearts of CTRL and KD mice subjected to endotoxin injection for 6 h. GAPDH was used as a loading control for total protein. $n = 6$ for all groups. * and #, $p < 0.05$ *versus* PBS CTRL; &, $p < 0.05$ *versus* PBS KD; $, $p < 0.05$ *versus* LPS CTRL. *G* and *H*, quantification of mtDNA by RT-PCR using primers targeted to mitochondrial cytochrome *b* (*CytB*, *G*) and mitochondrial cytochrome *c* (*CytC*, *H*) in hearts of CTRL and KD mice subjected to endotoxin injection for 6 h. $n = 4$ for all groups. *, $p < 0.05$ *versus* PBS CTRL; #, $p < 0.05$ *versus* PBS KD; &, $p < 0.05$ *versus* LPS WT. *I*, levels of mitochondrial hydrogen peroxide (ROS) in hearts of CTRL and KD mice subjected to endotoxin injection for 6 h were measured by Amplex Red assay. $n = 6$ for all groups. *, $p < 0.05$ *versus* PBS CTRL; #, $p < 0.05$ *versus* PBS KD; &, $p < 0.05$ *versus* LPS CTRL. *J*, levels of MPO in hearts of CTRL and KD mice subjected to endotoxin injection for 6 h were measured by MPO ELISA kit. $n = 4$ for all groups. *, $p < 0.05$ *versus* PBS CTRL; #, $p < 0.05$ *versus* PBS KD; &, $p < 0.05$ *versus* LPS CTRL.

degraded by mitophagy and is mediated by peroxisome proliferator-activated receptor-γ coactivator-1a (PGC-1a) (30). Therefore, we sought to determine the effects of TSG101 overexpression on these regulators of mitochondrial fission, fusion, and biogenesis in mouse hearts after LPS treatment. Under basal conditions, there were no significant alterations of Mfn1/2 and Drp1 but remarkable augmentation of PGC-1a levels in TG hearts compared with WT controls (Fig. 7, *A–E*). Of interest, upon LPS challenge, Mfn2 levels were significantly decreased in TG hearts, whereas Mfn1 levels were not altered compared with WT controls (Fig. 7, *A–C*). Importantly, Drp1 and PGC-1a levels were increased in both WT and TG hearts after LPS challenge; however, such increases in TG hearts were more significant than in WT hearts (Fig. 7, *A*, *D*, and *E*). Together, these results suggest that mitochondrial fusion is diminished but mitochondrial fission and biogenesis are augmented in TSG101-overexpressing hearts after endotoxin challenge.

Discussion

In this study, we identified a novel role of TSG101 in the regulation of mitophagy and endotoxin-induced myocardial depression. We observed that administration of endotoxin in mice augmented the activation of mitophagy and autophagic flux in mouse hearts, which correlated with elevation of TSG101 protein levels. Cardiac-specific overexpression of TSG101 in mice alleviated endotoxin-induced mortality, myocardial dysfunction, and inflammation. In addition, TSG101 transgenic hearts exhibited enhanced mitophagy and preservation of mitochondrial integrity. In contrast, LPS-induced mortality, cardiac dysfunction, and inflammation were aggravated in mice with cardiac-specific knockdown of TSG101. Reduction of TSG101 also caused inhibition of cardiac mitophagy after endotoxin challenge, leading to diminished mitochondrial structural integrity. Mechanistically, TSG101 interacted with Parkin in the cytosol under basal conditions, but this interaction was further enhanced and consequently translocated to mitochondria upon LPS treatment. Together, these findings suggest that TSG101-mediated protective effects in endotoxemic hearts are associated with enhanced mitophagy.

Currently, mitochondrial dysfunction is a critical feature of septic cardiomyopathy (11–14). Besides generation/biogenesis of new mitochondria, elimination of damaged mitochondria has been linked to recovery of cardiac function during sepsis in animal models (15, 16). It is well-known that each cardiomyocyte has a large volume of mitochondria and that mitochondria are essential for ATP generation (11–14). However, there are no therapies that are targeted to eliminate mitochondrial damage in septic patients. Furthermore, therapies developed to suppress inflammation in septic hearts have so far yielded negative outcomes (32). In fact, numerous studies have shown that defective mitophagy largely contributes to increased inflammatory response in various organs (33, 34). Injured mitochondria

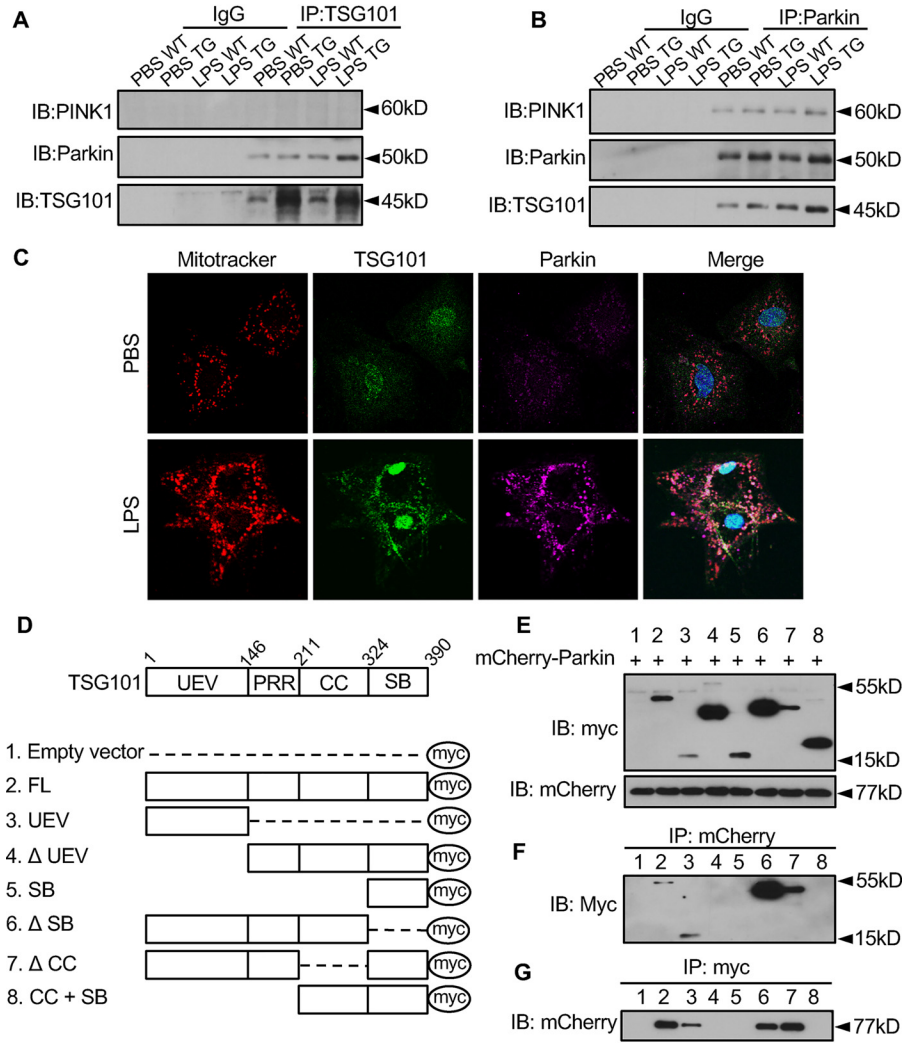

Figure 6. TSG101 interacts with and augments the function of Parkin in endotoxin-treated hearts. *A*, coimmunoprecipitation (*IP*) using anti-TSG101 and immunoblotting (*IB*) for PINK1, Parkin, and TSG101 in hearts of WT and TG mice subjected to PBS or LPS treatment for 6 h. $n = 4$ for all groups. *B*, coimmunoprecipitation using anti-Parkin and immunoblotting for PINK1, Parkin, and TSG101 in hearts of WT and TG mice subjected to PBS or LPS treatment for 6 h. $n = 4$ for all groups. *C*, immunofluorescence staining for mitochondria (*MitoTracker*), TSG101, and Parkin in NRCMs treated with either PBS or LPS (1 μg/ml) for 3 h. $n = 6$ plates for each group. *D*, full-length human TSG101 (domains: UEV, proline-rich region (*PRR*), coiled coil (*CC*), and steadiness box (*SB*)) and the indicated myc-tagged TSG101 truncated mutations. E, representative immunoblots showing the expression of mCherry-Parkin and TSG101 mutants in HEK293T cells. $n = 4$ independent experiments. *F*, coimmunoprecipitation using anti-mCherry and immunoblotting for anti-myc in HEK293T cells cotransfected with mCherry-Parkin and myc-tagged TSG101 mutants. $n = 4$ independent experiments. *G*, coimmunoprecipitation using anti-myc and immunoblotting for anti-mCherry in HEK293T cells cotransfected with mCherry-Parkin and myc-tagged TSG101 mutants. $n = 4$ independent experiments.

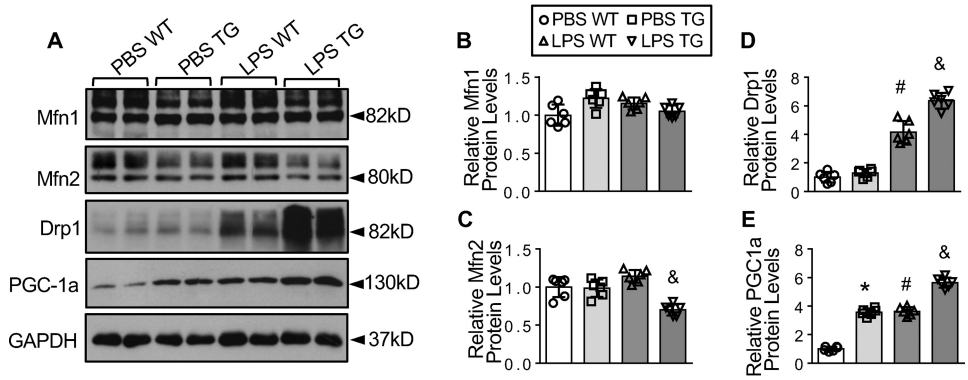

Figure 7. TSG101 promotes mitochondrial fission and biogenesis upon endotoxin challenge. *A–E*, Western blots and quantification analysis (*A*) showing the protein expression of Mfn1 (*B*), Mfn2 (*C*), Drp1 (*D*), and PGC-1a (*E*) in hearts of WT and TG mice subjected to endotoxin injection for 6 h. GAPDH was used as a loading control for total protein. $n = 6$ for each group. * and #, $p < 0.05$ *versus* PBS WT; &, $p < 0.05$ *versus* PBS TG; $, $p < 0.05$ *versus* LPS WT.

release various damage-associated molecular patterns (*i.e.* mtDNA and mtROS) that act to augment production of inflammatory cytokines intracellularly and, eventually, in neighboring immune cells (33, 34). For example, mtDNA released from damaged mitochondria has been demonstrated to bind to intracellular Toll-like receptor 9 (TLR9) and promote activation of NF-κB (35). Hence, targeting damaged mitochondria with mitophagy may be critical to eliminate the source of the inflammatory cytokine storm in septic hearts. Indeed, we observed in this study that enhancement of mitophagy by overexpression of TSG101 diminished the release of mtDNA and mtROS and, consequently, reduced the inflammatory response in endotoxemic hearts.

It is well accepted that general activation of autophagy in the heart can attenuate sepsis-induced cardiac dysfunction (36–39). Stimulation of autophagy with rapamycin in septic animals provides cardioprotection in terms of ATP production, lower inflammatory cytokine levels, and improved cardiac contractile performance (36–38). In addition, a recent study by Zhang *et al.* (39) showed that administration of melatonin enhanced autophagy in endotoxemic hearts and abrogated endotoxin-induced cardiac dysfunction and apoptosis. In the same vein, pharmacological activation of AMP-activated protein kinase/mTOR pathways activated autophagy and alleviated cardiac function impairment (40). More recently, Sun *et al.* (15) demonstrated that overexpression of Beclin-1, an important autophagy initiator, alleviates LPS-induced inflammation and cardiac dysfunction. These authors confirmed that Beclin-1-mediated protection in the endotoxemic heart was due to activation of the Parkin/PINK1 pathway. These previous observations consistently suggest that autophagy-mediated cardioprotection against sepsis may largely be due to removal of damaged and dysfunctional mitochondria. Similarly, beneficial effects induced by overexpression of TSG101 in endotoxemic hearts are associated with up-regulation of Parkin/PINK1 (Fig. 3).

Accumulating evidence indicates that endotoxin initially activates mitophagy and autophagy but that mitophagy gradually decreases in later stages of endotoxemia (15, 37). This initial activation of mitophagy may act as an adaptive and compensatory response to mitochondrial and cardiac dysfunction triggered by endotoxin. Although endotoxin could promote mitophagy and autophagic flux, this increase may not be enough to abrogate the effects of LPS-induced cardiac damage. Therefore, elevation of TSG101 in the heart may serve to augment mitophagy in the early stages of endotoxemia and may further provide continual activation of mitophagy and attenuation of endotoxin-induced cardiac dysfunction in later stages, leading to better survival outcomes (Fig. 2*C*). Mechanistically, TSG101 may act as a vehicle to shuttle Parkin to mitochondria, where Parkin may attract autophagy mediators (LC3) to transfer damaged mitochondria to the lysosome (Fig. 8). Given that knockdown of TSG101 does not affect the mRNA levels of Parkin but does diminish the protein levels of Parkin, we deduce that the interaction of TSG101 with Parkin contributes to the protein stability of Parkin. Although PINK1 levels were increased at basal levels, we did not see any evidence of interaction between TSG101 and PINK1 or any effects on mRNA

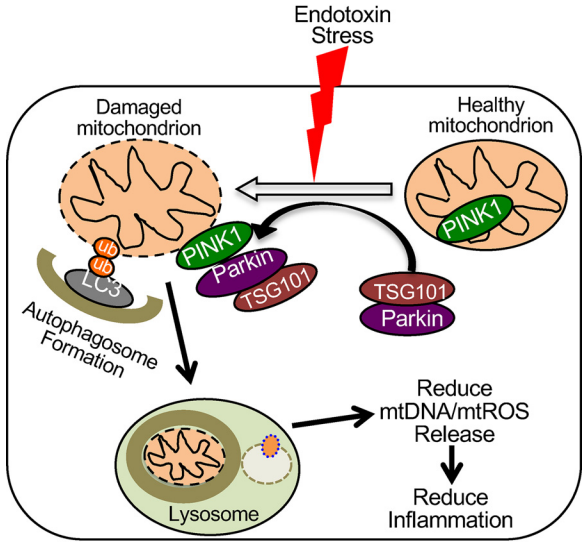

Figure 8. Scheme depicting TSG101-mediated protection against endotoxin-induced cardiac dysfunction. TSG101 is bound to Parkin in the cytosol under basal conditions. However, upon endotoxin stress stimuli, Parkin is translocated to mitochondria with the help of TSG101, where it interacts with PINK1. This action allows binding of ubiquitin, recruitment of the autophagy adaptor LC3, and formation of autophagosomes around the damaged mitochondria. The mitochondria are then targeted to the lysosome for degradation.

levels of PINK1. It is plausible that TSG101 may have an indirect effect on PINK1 through its interaction with Parkin. With respect to the discrepancy in basal cardiac function between TSG101-TG and -KD mice, in which TG mice showed enhanced contractile function and KD mice had normal cardiac phenotype, this could be due to constitutive overexpression of TSG101 in TG hearts (cardiac function was measured in 10- to 12-week old mice) and acute inducible knockdown of TSG101 in KD hearts (cardiac function was measured 1 week after the last tamoxifen injection).

In addition, there are several limitations to this study. First, this study focused on testing the role of TSG101 in endotoxin-induced cardiac injury. Although endotoxin is a major causative factor for Gram-negative bacterium–induced cardiomyopathy (4, 5), it will be interesting to investigate in the future whether TSG101 provides similar protection against true microbe-induced septic cardiomyopathy. Second, this study did not determine the long-term effects of overexpression of TSG101 in endotoxin-induced animal mortality and cardiac dysfunction. Previous work has demonstrated that increased levels of Parkin can protect against cardiac mitochondrial dysfunction and cardiac aging in 20-month-old mice (41). Considering that there are higher levels of Parkin in TSG101-TG hearts than in the WT, we could speculate that overexpression of TSG101 may have favorable long-term effects in aged mouse hearts. Finally, although we observed that overexpression of Tgs101 could enhance cardiac mitochondrial biogenesis, the underlying mechanisms remain to be clarified. As a matter of fact, recent studies have shown that Parkin positively regulates the expression of PGC-1a through activated ubiquitination and degradation of Parkin-interacting substrate, a transcriptional repressor of PGC-1a, in neurons (42, 43). Therefore, increased mitochondrial biogenesis in TSG101-TG hearts may be through enhanced expression of Parkin.

In conclusion, using gain- and loss-of-function approaches, we identify TSG101 as a new cardioprotective mediator to mitigate endotoxin-triggered cardiac impairment. Elevation of cardiac TSG101 is able to augment mitophagy in mouse hearts after LPS challenge, leading to a reduced inflammatory response and improved cardiac function and animal survival (Fig. 8). This study may provide new strategies for the treatment of endotoxemia.

Experimental procedures

Animals

Cardiac-specific TSG101-TG mice (Friend Virus B NIH background) were generated by the Transgenic Animal and Genome Editing Core at Cincinnati Children's Hospital Center as described previously (26). For this study, we selected to use the G line of the TSG101-TG mouse model, in which TSG101 was overexpressed by ~4-fold (26). The inducible heart-specific TSG101-KD mice were generated by crossing $TSG101^{fl/fl}$ female mice with αMHC-MerCreMer male mice to obtain male heterozygotes (MerCreMer-$TSG101^{fl/+}$) (26) (complete knockout of TSG101 in the mouse heart is lethal). The generation of floxed TSG101 allele mice ($TSG101^{fl/fl}$, 129/SvJ background) has been described previously (44). Mice expressing an inducible Cre recombinase transgene driven by the αMHC promoter (αMHC-MerCreMer) were purchased from The Jackson Laboratory (stock no. 005657). The MerCreMer-$TSG101^{fl/+}$ male offspring were injected at 8–9 weeks of age with tamoxifen (Sigma, 30 μg/g) daily, for 3 consecutive days, to induce knockdown of cardiac TSG101, as described previously (26). Tamoxifen-injected $TSG101^{fl/+}$ male mice were used as CTRL mice. TSG101-KD and CTRL mice were utilized for experiments 1 week after the last tamoxifen injection.

All mice used in this study were maintained and bred in the Division of Laboratory Animal Resources at the University of Cincinnati Medical Center. Animal experiments conformed to the Guidelines for the Care and Use of Laboratory Animals prepared by the National Academy of Sciences, published by the National Institutes of Health, and were approved by the University of Cincinnati Animal Care and Use Committee.

Mouse model of endotoxemia

10- to 12-week-old male mice were injected i.p. with *Escherichia coli* LPS (Sigma) at 10 μg/g to induce endotoxemia. Mice were injected with PBS as a control. The heart tissues were collected at 0, 6, and 24 h for Western blotting, qRT-PCR and quantification of mtDNA, mtROS, and cardiac MPO levels. Serum was collected 6 h after LPS injection for ELISA. Cardiac function in mice was measured by echocardiography 12 h after endotoxin challenge. Survival analysis after LPS injection was monitored every 6 h up to 5 days.

Western blotting and ELISA for cytokines and myeloperoxidases

Total proteins were extracted from hearts using NP40 lysis buffer (cOmplete™ Mini) supplemented with protease inhibitor mixture (Roche) according to the manufacturer's instructions. Mitochondrion and cytosol fractions were isolated from freshly harvested mouse heart tissue using the Mitochondria Isolation Kit for Tissue (Thermo Fisher) according to the manufacturer's protocol. The concentrations of total, cytosolic, and mitochondrial protein were determined by protein assay reagent (Bio-Rad). Samples (25–100 μg) were loaded to SDS-PAGE as discussed in detail elsewhere (45). The dilutions and sources of the primary antibodies used in this study were as follows: mouse anti-TSG101 (Santa Cruz, 1:1000), PINK1 (Cell Signaling, 1:1000), Parkin (Cell Signaling, 1:1000), LC3 (Cell Signaling, 1:500), Mfn1 (Abcam, 1:1000), Mfn2 (Abcam, 1:1000), Drp1 (Cell Signaling, 1:500), and PGC-1a (Proteintech, 1:1000). GAPDH (Cell Signaling, 1:1000) was used as a loading control for total and cytosolic protein levels. TOM20 (Cell Signaling, 1:1000) was used a loading control for mitochondrial protein. Western blot bands were quantified by MultiImage II (AlphaInnotech). The relative target protein levels were normalized to GAPDH. Serum TNFα and IL-6 levels were determined by commercially available kits (Biolegend) according to the manufacturer's protocols. MPO levels were determined in heart homogenates using a commercial MPO ELISA kit (Abnova) by following the manufacturer's instructions.

qRT-PCR analysis and measurement of mtDNA

Total RNA from heart samples was isolated using the miRNeasy Mini Kit (Qiagen). The quality and concentration of RNA was determined using the NanoDrop 2000 system (Thermo Fisher Scientific). The miScript PCR Starter Kit (Qiagen) was used to generate complementary DNA according to the manufacturer's protocol. qRT-PCR was performed using SYBR GreenER qPCR SuperMix (Invitrogen) in a total reaction volume of 20 μl. All primers were synthesized by Integrated DNA Technologies. The primer sequences for qRT-PCR analysis are listed in Table S3. Relative -fold expression for target genes was calculated by the $2^{-\Delta\Delta Ct}$ method relative to the housekeeping gene GAPDH.

Total DNA was isolated from heart tissues using the DNeasy Blood and Tissue kit (Qiagen). The subsequent PCR analysis for quantification of cardiac mtDNA was similar to the qRT-PCR protocols described above. mtDNA was quantified relative to nuclear DNA. The primer sequences for measurement of mtDNA are listed in Table S3.

Quantification of mtROS

The mitochondrial fraction was isolated from freshly harvested heart tissue using the Mitochondria Isolation Kit for Tissue (Thermo Fisher) as described above. The cardiac mitochondrial fraction was then subjected to evaluation of ROS using the Amplex™ Red Hydrogen Peroxide/Peroxidase Assay Kit (Invitrogen), following the manufacturer's instructions.

Echocardiography

Cardiac function was assessed *in vivo* using trans-thoracic M-model echocardiography (Vevo2100 Imaging System, Visualsonics) with a 15-MHz probe as described previously (26). Briefly, mice underwent anesthesia by isoflurane (1.5–2.0%). Parasternal long axis and short axis images were taken and analyzed with VevoStrain (Vevo 2100, v1.1.7 B1455) software.

Isolation of neonatal rat cardiomyocytes and immunofluorescence staining

Rat neonates (1–3 days old) were anesthetized in an ice bath, and the hearts were excised under sterile conditions. NRCMs were isolated using the neonatal cardiomyocyte isolation system (Worthington Biochemical Corp.), following the manufacturer's procedures. NRCMs were cultured in DMEM supplemented with 2% FBS and 1% antibiotics (penicillin and streptomycin). NRCMs were seeded in 3.8-cm^2 culture wells for 48 h. Subsequently, NRCMs were treated with 1 μg/ml LPS or an equivalent volume of PBS for 3 h, followed by addition of 200 nM MitoTracker (Cell Signaling) for 15 min. NRCMs were then washed twice with PBS and fixed with cold methanol for 10 min at −20 °C. After fixing, NRCMs underwent permeabilization and blocking in PBS (5% BSA and 0.3% Triton) solution for 1 h at room temperature, and then cells were incubated with mouse anti-Parkin antibody (Cell Signaling, 1:100 dilution in PBS with 1% BSA) and rabbit anti-TSG101 (Proteintech, 1:100 dilution in PBS with 1% BSA) at 4 °C overnight. The next day, NRCMs were washed and stained with Alexa Fluor 649 goat anti-mouse IgG (Invitrogen, 1:500) and Alexa Fluor 488 goat anti-mouse IgG (Invitrogen, 1:500) at room temperature for 1 h. Cells were examined using confocal microscopy.

Transfection of adenoviruses, exosome isolation, and treatment of RAW264.7 macrophages

NRCMs were isolated and cultured in 2% FBS and 1% antibiotics as described above. The cells were transfected with Ad.TSG101. Ad.TSG101 was acquired from the laboratory of Dr. G. Paolo Dotto (Massachusetts General Hospital and Harvard Medical School). NRCMs were transfected with Ad.GFP as controls. Supernatants from cultured Ad.GFP and Ad.TSG101 NRCMs were collected on ice and centrifuged at 3000 × *g* for 20 min to remove any dead cells, followed by centrifugation at 10,000 × *g* for 30 min at 4 °C to remove any cellular debris. Thereafter, supernatants were collected and filtered through 0.22-μm filters, followed by ultracentrifugation at 100,000 × *g* (Ti-45 rotor) for 2 h at 4 °C to pellet exosomes. The exosome pellet was finally washed once with PBS. The exosome protein concentration was determined by protein assay reagent (Bio-Rad). Expression of the exosome marker (CD63) was determined by Western blotting. The size and quality of exosomes was assessed by dynamic light scattering using a particle and molecular size analyzer (Zetasizer Nano ZS, Malvern Instruments).

Exosomes isolated from Ad.TSG101-transfected NRCMs (TSG101-exo) and Ad.GFP-transfected NRCMs (GFP-exo) were treated at a dose of 2 μg/ml in mouse macrophage cell line RAW264.7 (ATCC) for 24 h before macrophages were stimulated with PBS or LPS (0.5 μg/ml) for 6 h. Cells were then collected for Western blotting, and culture supernatants were harvested to determine levels of cytokines by ELISA.

Coimmunoprecipitation analysis

500 mg of mouse heart homogenate was solubilized in 1 ml of NP40 lysis buffer (with protease inhibitor mixture) and precleared in 50 μl of protein A/G–agarose beads (Cell Signaling) for 1 h at 4 °C on a rotary wheel. The mixture was then incubated with 1 μg of the corresponding primary antibodies at 4 °C overnight on a rotary wheel. Immunoprecipitates were collected and washed five times in NP40 lysis buffer. Immunoprecipitates were resolved in 2× Laemmli sample buffer and boiled at 95 °C for 5 min. Eluted proteins from the antibody–bead conjugate were subjected to SDS-PAGE.

TSG101–Parkin interaction analysis

The different truncations of myc-tagged human TSG101 were a gift from Dr. Tzu-Hao Cheng (National Yang-Ming University) and were generated as described previously (46). mCherry-Parkin was a gift from Dr. Richard Youle (Addgene plasmid 23956). The TSG101–Parkin interaction analysis was performed in HEK293T cells by cotransfection of mCherry-Parkin and the respective myc-TSG101 truncates, utilizing Lipofectamine 3000 transfection reagent (Thermo Fisher). Cells were collected after 72-h culture for Western blotting and coimmunoprecipitation analysis as described above.

Statistical analysis

Data were expressed as means ± S.D. Significance was determined by Student's *t* test and one- or two-way analysis of variance to determine differences within groups where appropriate. A log-rank test was used to determine statistical significance for the survival analysis. $p < 0.05$ was considered statistically significant.

Author contributions—K. E. and G.-C. F. conceptualization; K. E., X. W., W. H., S. D., G. G., X. M., and Y. L. data curation; K. E., W. H., G. G., Y. L., and G.-C. F. formal analysis; K. E. and G.-C. F. funding acquisition; K. E., X. W., W. H., S. D., G. G., X. M., Y. L., E. G. K., and Y. W. investigation; K. E., X. W., W. H., S. D., G. G., X. M., and Y. L. methodology; K. E. and G.-C. F. writing-original draft; K. E., E. G. K., Y. W., and G.-C. F. writing-review and editing; X. W., E. G. K., Y. W., and G.-C. F. supervision; X. W., E. G. K., Y. W., and G.-C. F. validation; Y. W. and G.-C. F. resources; G.-C. F. project administration.

References

1. Singer, M., Deutschman, C. S., Seymour, C. W., Shankar-Hari, M., Annane, D., Bauer, M., Bellomo, R., Bernard, G. R., Chiche, J. D., Coopersmith, C. M., Hotchkiss, R. S., Levy, M. M., Marshall, J. C., Martin, G. S., Opal, S. M., *et al.* (2016) The third international consensus definitions for sepsis and septic shock (Sepsis-3). *JAMA* **315,** 801–810 CrossRef Medline
2. Landesberg, G., Gilon, D., Meroz, Y., Georgieva, M., Levin, P. D., Goodman, S., Avidan, A., Beeri, R., Weissman, C., Jaffe, A. S., and Sprung, C. L. (2012) Diastolic dysfunction and mortality in severe sepsis and septic shock. *Eur. Heart J.* **33,** 895–903 CrossRef Medline
3. Havaldar, A. A. (2018) Evaluation of sepsis induced cardiac dysfunction as a predictor of mortality. *Cardiovasc. Ultrasound* **16,** 31 CrossRef Medline
4. Flesch, M., Kilter, H., Cremers, B., Laufs, U., Südkamp, M., Ortmann, M., Müller, F. U., and Böhm, M. (1999) Effects of endotoxin on human myocardial contractility involvement of nitric oxide and peroxynitrite. *J. Am. Coll. Cardiol.* **33,** 1062–1070 CrossRef Medline
5. Hobai, I. A., Aziz, K., Buys, E. S., Brouckaert, P., Siwik, D. A., and Colucci, W. S. (2016) Distinct myocardial mechanisms underlie cardiac dysfunction in endotoxemic male and female mice. *Shock* **46,** 713–722 CrossRef Medline
6. Liu, Y.-C., Yu, M.-M., Shou, S.-T., and Chai, Y.-F. (2017) Sepsis-induced cardiomyopathy: mechanisms and treatments. *Front. Immunol.* **8,** 1021 CrossRef Medline

7. Piquereau, J., Caffin, F., Novotova, M., Lemaire, C., Veksler, V., Garnier, A., Ventura-Clapier, R., and Joubert, F. (2013) Mitochondrial dynamics in the adult cardiomyocytes: which roles for a highly specialized cell? *Front. Physiol.* **4,** 102 Medline
8. Ni, H. M., Williams, J. A., and Ding, W. X. (2015) Mitochondrial dynamics and mitochondrial quality control. *Redox. Biol.* **4,** 6–13 CrossRef Medline
9. Chistiakov, D. A., Shkurat, T. P., Melnichenko, A. A., Grechko, A. V., and Orekhov, A. N. (2018) The role of mitochondrial dysfunction in cardiovascular disease: a brief review. *Ann. Med.* **50,** 121–127 Medline
10. Siasos, G., Tsigkou, V., Kosmopoulos, M., Theodosiadis, D., Simantiris, S., Tagkou, N. M., Tsimpiktsioglou, A., Stampouloglou, P. K., Oikonomou, E., Mourouzis, K., Philippou, A., Vavuranakis, M., Stefanadis, C., Tousoulis, D., and Papavassiliou, A. G. (2018) Mitochondria and cardiovascular diseases: from pathophysiology to treatment. *Ann. Transl. Med.* **6,** 256–256 CrossRef Medline
11. Soriano, F. G., Nogueira, A. C., Caldini, E. G., Lins, M. H., Teixeira, A. C., Cappi, S. B., Lotufo, P. A., Bernik, M. M., Zsengellér, Z., Chen, M., and Szabó, C. (2006) Potential role of poly(adenosine 5′-diphosphate-ribose) polymerase activation in the pathogenesis of myocardial contractile dysfunction associated with human septic shock. *Crit. Care Med.* **34,** 1073–1079 CrossRef Medline
12. Vanasco, V., Saez, T., Magnani, N. D., Pereyra, L., Marchini, T., Corach, A., Vaccaro, M. I., Corach, D., Evelson, P., and Alvarez, S. (2014) Cardiac mitochondrial biogenesis in endotoxemia is not accompanied by mitochondrial function recovery. *Free Radic. Biol. Med.* **77,** 1–9 CrossRef Medline
13. Makrecka-Kuka, M., Korzh, S., Vilks, K., Vilskersts, R., Cirule, H., Dambrova, M., and Liepinsh, E. (2019) Mitochondrial function in the kidney and heart, but not the brain, is mainly altered in an experimental model of endotoxaemia. *Shock* CrossRef Medline
14. Tavener, S. A., Long, E. M., Robbins, S. M., McRae, K. M., Van Remmen, H., and Kubes, P. (2004) Immune cell Toll-like receptor 4 is required for cardiac myocyte impairment during endotoxemia. *Circ. Res.* **95,** 700–707 CrossRef Medline
15. Sun, Y., Yao, X., Zhang, Q.-J., Zhu, M., Liu, Z.-P., Ci, B., Xie, Y., Carlson, D., Rothermel, B. A., Sun, Y., Levine, B., Hill, J. A., Wolf, S. E., Minei, J. P., and Zang, Q. S. (2018) Beclin-1-Dependent autophagy protects the heart during sepsis. *Circulation* **138,** 2247–2262 CrossRef Medline
16. Hickson-Bick, D. L., Jones, C., and Buja, L. M. (2008) Stimulation of mitochondrial biogenesis and autophagy by lipopolysaccharide in the neonatal rat cardiomyocyte protects against programmed cell death. *J. Mol. Cell. Cardiol.* **44,** 411–418 CrossRef Medline
17. Kitada, T., Asakawa, S., Hattori, N., Matsumine, H., Yamamura, Y., Minoshima, S., Yokochi, M., Mizuno, Y., and Shimizu, N. (1998) Mutations in the parkin gene cause autosomal recessive juvenile parkinsonism. *Nature* **392,** 605–608 CrossRef Medline
18. Valente, E. M., Abou-Sleiman, P. M., Caputo, V., Muqit, M. M., Harvey, K., Gispert, S., Ali, Z., Del Turco, D., Bentivoglio, A. R., Healy, D. G., Albanese, A., Nussbaum, R., González-Maldonado, R., Deller, T., Salvi, S., *et al.* (2004) Hereditary early-onset parkinsons disease caused by mutations in PINK1. *Science* **304,** 1158–1160 CrossRef Medline
19. Pickles, S., Vigié, P., and Youle, R. J. (2018) Mitophagy and quality control mechanisms in mitochondrial maintenance. *Curr. Biol.* **28,** R170–R185 CrossRef Medline
20. Piquereau, J., Godin, R., Deschênes, S., Bessi, V. L., Mofarrahi, M., Hussain, S. N., and Burelle, Y. (2013) Protective role of PARK2/Parkin in sepsis-induced cardiac contractile and mitochondrial dysfunction. *Autophagy* **9,** 1837–1851 CrossRef Medline
21. Zhu, G., Gilchrist, R., Borley, N., Chng, H. W., Morgan, M., Marshall, J. F., Camplejohn, R. S., Muir, G. H., and Hart, I. R. (2004) Reduction of TSG101 protein has a negative impact on tumor cell growth. *Int. J. Cancer* **109,** 541–547 CrossRef Medline
22. Moberg, K. H., Schelble, S., Burdick, S. K., and Hariharan, I. K. (2005) Mutations in erupted, the *Drosophila* ortholog of mammalian tumor susceptibility gene 101, elicit non-cell-autonomous overgrowth. *Dev. Cell* **9,** 699–710 CrossRef Medline
23. Slagsvold, T., Pattni, K., Malerød, L., and Stenmark, H. (2006) Endosomal and non-endosomal functions of ESCRT proteins. *Trends Cell Biol.* **16,** 317–326 CrossRef Medline
24. Filimonenko, M., Stuffers, S., Raiborg, C., Yamamoto, A., Malerød, L., Fisher, E. M., Isaacs, A., Brech, A., Stenmark, H., and Simonsen, A. (2007) Functional multivesicular bodies are required for autophagic clearance of protein aggregates associated with neurodegenerative disease. *J. Cell Biol.* **179,** 485–500 CrossRef Medline
25. Majumder, P., and Chakrabarti, O. (2015) Mahogunin regulates fusion between amphisomes/MVBs and lysosomes via ubiquitination of TSG101. *Cell Death Dis.* **6,** e1970 CrossRef Medline
26. Essandoh, K., Deng, S., Wang, X., Jiang, M., Mu, X., Peng, J., Li, Y., Peng, T., Wagner, K.-U., Rubinstein, J., and Fan, G.-C. (2019) Tsg101 positively regulates physiologic-like cardiac hypertrophy through FIP3-mediated endosomal recycling of IGF-1R. *FASEB J.* **33,** 7451–7466 CrossRef Medline
27. Wang, X., Gu, H., Huang, W., Peng, J., Li, Y., Yang, L., Qin, D., Essandoh, K., Wang, Y., Peng, T., and Fan, G.-C. (2016) Hsp20-mediated activation of exosome biogenesis in cardiomyocytes improves cardiac function and angiogenesis in diabetic mice. *Diabetes* **65,** 3111–3128 CrossRef Medline
28. Dan Dunn, J., Alvarez, L. A., Zhang, X., and Soldati, T. (2015) Reactive oxygen species and mitochondria: a nexus of cellular homeostasis. *Redox Biol.* **6,** 472–485 CrossRef Medline
29. Jiang, Y., Ou, Y., and Cheng, X. (2013) Role of TSG101 in cancer. *Front. Biosci.* **18,** 279–288 CrossRef Medline
30. Ong, S.-B., Kalkhoran, S. B., Hernández-Reséndiz, S., Samangouei, P., Ong, S.-G., and Hausenloy, D. J. (2017) Mitochondrial-shaping proteins in cardiac health and disease: the long and the short of it! *Cardiovasc, Drugs Ther.* **31,** 87–107 CrossRef Medline
31. Burman, J. L., Pickles, S., Wang, C., Sekine, S., Vargas, J. N. S., Zhang, Z., Youle, A. M., Nezich, C. L., Wu, X., Hammer, J. A., and Youle, R. J. (2017) Mitochondrial fission facilitates the selective mitophagy of protein aggregates. *J. Cell Biol.* **216,** 3231–3247 CrossRef Medline
32. Russell, J. A., and Walley, K. R. (2013) Update in sepsis 2012. *Am. J. Respir. Crit. Care Med.* **187,** 1303–1307 CrossRef Medline
33. Jansen, M. P. B., Pulskens, W. P., Butter, L. M., Florquin, S., Juffermans, N. P., Roelofs, J. J. T. H., and Leemans, J. C. (2018) Mitochondrial DNA is released in urine of SIRS Patients with acute kidney injury and correlates with severity of renal dysfunction. *Shock* **49,** 301–310 CrossRef Medline
34. Gkikas, I., Palikaras, K., and Tavernarakis, N. (2018) The role of mitophagy in innate immunity. *Front. Immunol.* **9,** 1283 CrossRef Medline
35. Rodríguez-Nuevo, A., Díaz-Ramos, A., Noguera, E., Díaz-Sáez, F., Duran, X., Muñoz, J. P., Romero, M., Plana, N., Sebastián, D., Tezze, C., Romanello, V., Ribas, F., Seco, J., Planet, E., Doctrow, S. R., *et al.* (2018) Mitochondrial DNA and TLR9 drive muscle inflammation upon Opa1 deficiency. *EMBO J.* **37,** e96553 Medline
36. Takahashi, W., Watanabe, E., Fujimura, L., Watanabe-Takano, H., Yoshidome, H., Swanson, P. E., Tokuhisa, T., Oda, S., and Hatano, M. (2013) Protective role of autophagy in mouse cecal ligation and puncture-induced sepsis model. *Crit. Care* **17,** R160 CrossRef Medline
37. Hsieh, C.-H., Pai, P.-Y., Hsueh, H.-W., Yuan, S.-S., and Hsieh, Y.-C. (2011) Complete induction of autophagy is essential for cardioprotection in sepsis. *Ann. Surg.* **253,** 1190–1200 CrossRef Medline
38. Wang, H., Cui, N., Han, W., Su, L.-X., Long, Y., and Liu, D.-W. (2018) Accelerated autophagy of cecal ligation and puncture-induced myocardial dysfunction and its correlation with mammalian target of rapamycin pathway in rats. *Chin. Med. J.* **131,** 1185–1190 CrossRef Medline
39. Zhang, W.-X., He, B.-M., Wu, Y., Qiao, J.-F., and Peng, Z.-Y. (2019) Melatonin protects against sepsis-induced cardiac dysfunction by regulating apoptosis and autophagy via activation of SIRT1 in mice. *Life Sci.* **217,** 8–15 CrossRef Medline
40. Zhang, J., Zhao, P., Quan, N., Wang, L., Chen, X., Cates, C., Rousselle, T., and Li, J. (2017) The endotoxemia cardiac dysfunction is attenuated by AMPK/mTOR signaling pathway regulating autophagy. *Biochem. Biophys. Res. Commun.* **492,** 520–527 CrossRef Medline

41. Hoshino, A., Mita, Y., Okawa, Y., Ariyoshi, M., Iwai-Kanai, E., Ueyama, T., Ikeda, K., Ogata, T., and Matoba, S. (2013) Cytosolic p53 inhibits Parkin-mediated mitophagy and promotes mitochondrial dysfunction in the mouse heart. *Nat. Commun.* **4,** 2308 CrossRef Medline
42. Stevens, D. A., Lee, Y., Kang, H. C., Lee, B. D., Lee, Y.-I., Bower, A., Jiang, H., Kang, S.-U., Andrabi, S. A., Dawson, V. L., Shin, J.-H., and Dawson, T. M. (2015) Parkin loss leads to PARIS-dependent declines in mitochondrial mass and respiration. *Proc. Natl. Acad. Sci. U.S.A.* **112,** 11696–11701 CrossRef Medline
43. Zheng, L., Bernard-Marissal, N., Moullan, N., D'Amico, D., Auwerx, J., Moore, D. J., Knott, G., Aebischer, P., and Schneider, B. L. (2017) Parkin functionally interacts with PGC-1α to preserve mitochondria and protect dopaminergic neurons. *Hum. Mol. Genet.* **26,** 582–598 Medline
44. Wagner, K.-U., Krempler, A., Qi, Y., Park, K., Henry, M. D., Triplett, A. A., Riedlinger, G., Rucker, E. B., 3rd., and Hennighausen, L. (2003) Tsg101 is essential for cell growth, proliferation, and cell survival of embryonic and adult tissues. *Mol. Cell Biol.* **23,** 150–162 CrossRef Medline
45. Peng, J., Li, Y., Wang, X., Deng, S., Holland, J., Yates, E., Chen, J., Gu, H., Essandoh, K., Mu, X., Wang, B., McNamara, R. K., Peng, T., Jegga, A. G., Liu, T., *et al.* (2018) An Hsp20-FBXO4 axis regulates adipocyte function through modulating PPARγ ubiquitination. *Cell Rep.* **23,** 3607–3620 CrossRef Medline
46. Lin, Y. S., Chen, Y. J., Cohen, S. N., and Cheng, T. H. (2013) Identification of TSG101 functional domains and p21 loci required for TSG101-mediated p21 gene regulation. *PLoS ONE* **8,** e79674 CrossRef Medline